Hindawi
Journal of Applied Mathematics
Volume 2021, Article ID 6406274, 17 pages
https://doi.org/10.1155/2021/6406274

Research Article

The COVID-19 Model with Partially Recovered Carriers

T. S. Faniran,[1] E. A. Bakare ,[2,3] and A. O. Falade[4]

[1]*Department of Computer Science, Lead City University, Ibadan, Nigeria*
[2]*Modelling, Simulation and Data Science Network, Africa (MOD-SIMUD.net, Africa), Nigeria*
[3]*Department of Mathematics, Federal University Oye Ekiti, Ekiti State, Nigeria*
[4]*Department of Mathematics, African Institute for Mathematical Sciences, Mbour, Senegal*

Correspondence should be addressed to E. A. Bakare; emmanuel.bakare@fuoye.edu.ng

Received 4 July 2020; Revised 18 February 2021; Accepted 9 March 2021; Published 9 July 2021

Academic Editor: Ali R. Ashrafi

Novel coronavirus (COVID-19) has been spreading and wreaking havoc globally, despite massive efforts by the government and World Health Organization (WHO). Consideration of partially recovered carriers is hypothesized to play a leading role in the persistence of the disease and its introduction to new areas. A model for transmission of COVID-19 by symptomless partially recovered carriers is proposed and analysed. It is shown that key parameters can be identified such that below a threshold level, built on these parameters, the epidemic tends towards extinction, while above another threshold, it tends towards a nontrivial epidemic state. Moreover, optimal control analysis of the model, using Pontryagin's maximum principle, is performed. The optimal controls are characterized in terms of the optimality system and solved numerically for several scenarios. Numerical simulations and sensitivity analysis of the basic reproduction number, R_c, indicate that the disease is mainly driven by parameters involving the partially recovered carriers rather than symptomatic ones. Moreover, optimal control analysis of the model, using Pontryagin's maximum principle, is performed. The optimal controls were characterized in terms of the optimality system and solved numerically for several scenarios. Numerical simulations were explored to illustrate our theoretical findings, scenarios were built, and the model predicted that social distancing and treatment of the symptomatic will slow down the epidemic curve and reduce mortality of COVID-19 given that there is an average adherence to social distancing and effective treatment are administered.

1. Introduction

Coronavirus is one of the major pathogens that primarily targets the human respiratory system. The previous outbreak of coronaviruses include the severe acute respiratory syndrome (SARS), which occurred in 2003 in Mainland China [1], the Middle East respiratory Syndrome (MERS) in 2012 in Saudi Arabia [2], and the MERS outbreak in 2015 in South Korea [3]. In late December 2019, a cluster of patients was admitted to hospitals with an initial diagnosis of pneumonia of an unknown etiology. These patients were etiologically linked to seafood and wet animal wholesale market in Wuhan, the capital city of the Hubei province, China [4]. Early reports predicted the onset of a potential coronavirus outbreak and estimated the reproduction number to be significantly larger than 1 (ranges from 2.24 to 3.58) [5].

A report published in Nature revealed that Chinese health authorities concluded that as of February 7, 2020, there have been 31,161 people who have contracted the infection in China and more than 630 people have died of the infection [6] [http://www.nature.com/articles/d41586-020-00154]. Also, the World Health Organization (WHO) reported 51,174 confirmed cases including 15,384 severe cases and 1,666 death cases in China. At the time of preparing this manuscript, the number of cases (March 7, 2020) has passed 100,000 worldwide, reported by Euronews.

The most common symptoms at the onset of COVID-19 illness are fever, cough, and fatigue, while other symptoms include sputum production, headache, hemoptysis, diarrhea, and lymphopenia [7].

Mathematical models for dynamics of the transmission and control of COVID-19 have been developed to gain

insights on the disease dynamics. Also, as recognized by the WHO [8], mathematical models, especially those who are timely, play a key role in informing evidence-based decisions by health decision and policy makers. Only a few mathematical models have so far been publicly released, to the best of our knowledge. Notably among these studies are [9–18].

This study has an important difference from those reported above, in that it presents a mathematical model that considers a proportion of infectious patients who recover partially. These proportions may still be virus carriers. According to a new study developed by Lan et al. [19], they followed four medical professionals ages 30 to 36 years who developed COVID-19 and were treated at Wuhan University's Zhongnan Hospital in China between Jan. 1 and Feb. 15. All of the individuals recovered, and only one was hospitalized during the illness. The patients were treated with oseltamivir, better known under the brand name of Tamiflu, an antiviral drug. The patients were considered recovered after their symptoms. After recovery, the patients were asked to quarantine themselves at home for five days. They continued to undergo throat swabs for the coronavirus after five days for up to 13 days postrecovery. The results showed that every test between day 5 and day 13 was positive for the virus. Also, a paper published by Pappas [20] gave an instance of a Japanese patient who recovered from COVID-19 and then became ill with the disease for a second time. Pappas [20] explained further that one possibility is that the patient's immune system did not fight off the virus completely as it began to replicate inside her lung. These findings suggested that at least a proportion of infectious individuals did not recover fully from the disease because a small concentration of the virus might still be in their system which began to replicate. Hence, these groups are classified as partially recovered carriers, as they are virus carriers. This is a new finding that has not been modelled mathematically. Therefore, the present study bridges this knowledge gap.

The remaining part of this paper is organized as follows: in Section 2, model description and formulation are presented. Detailed stability of disease-free equilibrium points is analysed in Section 3. Sections 4 presents the sensitivity analysis of the model parameters while in Section 5, we provide the optimal control problem, its formulation, optimal strategies, proof of existence, and necessary conditions for optimal control. Section 6 provides the numerical simulations of the formulated model. Finally, Section 7 gives the overall concluding remarks of the study.

2. Mathematical Formulation of the COVID-19 Model

In this section, a model for the spread of COVID-19 in human and vector population is formulated. The total human population denoted by N_H, is partitioned into five classes, namely, the susceptible individual S_H, the exposed individual E_H, the infectious individual I_H, the partially recovered carriers P_C, and the fully recovered individuals R_H, so that $N_H = S_H + E_H + I_H + P_C + R_H$.

2.1. Assumptions of the Model. The following assumptions were made in order to formulate the equations of the model:

(a) Containment rate, c_m, is introduced into the susceptible population

(b) SARS-COV-2 can persist in the body for at least two weeks after symptoms of the disease clear up [20]

(c) Infectious patients whose immune system fights off the virus completely with no single virus left progress to the fully recovered class

(d) Infectious patients whose immune system does not fight off the virus completely (i.e., low level of the virus are still present in their system) progress to the partially recovered carrier class

(e) Reverse transcription polymerase chain reaction (RT-PCR) may not be able to detect the presence of a very low level of the virus in the system of partially recovered carriers at the time that they are discharged from the hospital

(f) Virus begins to replicate inside the lungs of the partially recovered carriers again [20]

(g) Partially recovered carriers are contagious but show mild or no symptoms

(h) Individuals in the partially recovered carrier class can also recover from COVID-19, but with a significantly slow rate

Our model includes a net inflow of susceptible individuals into a region at a rate, λ_h per unit time. This parameter includes new births, immigration, and emigration. The susceptible individuals acquire COVID-19 through contact with either the infectious individuals or partially recovered carriers at rates α and β. Also, the susceptible population is reduced by containment rate, c_m. The proportion of the infectious individuals become partially recovered carriers at a rate $(1-\varepsilon)$. Individuals in the partially recovered carrier class recover fully from the disease at a slower rate $\psi_2\eta$.

Applying the assumptions, nomenclature of parameters, and definitions of variables, the following system of ordinary differential equations is formulated:

$$\frac{dS_H}{dt} = \lambda_h - \alpha S_H I_H - \beta S_H P_C - c_m S_H, \tag{1}$$

$$\frac{dE_H}{dt} = \alpha S_H I_H + \beta S_H P_C - \theta E_H, \tag{2}$$

$$\frac{dI_H}{dt} = \theta E_H - \gamma I_H - \psi_1 I_H - \tau I_H, \tag{3}$$

$$\frac{dP_C}{dt} = (1-\varepsilon)\tau I_H - \psi_2 \eta P_C, \tag{4}$$

$$\frac{dR_H}{dt} = \varepsilon\tau I_H + \psi_1 I_H + \psi_2 \eta P_C, \tag{5}$$

with initial conditions

$$\begin{aligned} S_H(0) &= S_h^0 > 0, \\ E_H(0) &= E_H^0, \\ I_H(0) &= I_H^0(0) > 0, \\ P_C(0) &= P_C^0(0), \\ R_H(0) &= R_H^0(0) > 0, \end{aligned} \tag{6}$$

where the model parameters are nonnegative.

Remark 1. We restructure and modify the model to have more insightful information. However, it has not in any way changed the research focus.

The first four equations, i.e., (1), (2), (3), and (4), are independent of the compartments R_H, i.e., (5). Therefore, after decoupling the equations for R_H from models (1), (2), (3), (4), and (5), we devote analyses on the remaining equations of (1), (2), (3), and (4) which becomes

$$\frac{dS_H}{dt} = \lambda_h - \alpha S_H I_H - \beta S_H P_C - c_m S_H, \tag{7}$$

$$\frac{dE_H}{dt} = \alpha S_H I_H + \beta S_H P_C - \theta E_H, \tag{8}$$

$$\frac{dI_H}{dt} = \theta E_H - \gamma I_H - \psi_1 I_H - \tau I_H, \tag{9}$$

$$\frac{dP_C}{dt} = (1-\varepsilon)\tau I_H - \psi_2 \eta P_C, \tag{10}$$

where the disease-free equilibrium point is $E_0 = (S_H, E_H, I_H, P_C) = ((\lambda_h/c_m), 0, 0, 0)$.

3. Stability Analysis

3.1. Local Stability of Disease-Free Equilibrium Solution. Using the next-generation operator approach of Diekmann et al., [21], the effective basic reproduction number associated with disease-free equilibrium, E_0, and denoted by R_c, is obtained as

$$R_c = \frac{\alpha S_0 \psi_2 \eta + \beta S_0 (1-\varepsilon)\tau}{\psi_2 \eta B_T}, \tag{11}$$

where

$$S_0 = \frac{\lambda_h}{c_m}. \tag{12}$$

Clearly, the disease-free equilibrium is locally asymptotically stable if $R_c < 1$. To see this, we obtain the Jacobian matrix of systems (7), (8), (9), and (10) evaluated at E_0:

$$J_{E_0} = \begin{bmatrix} -c_m & 0 & -\alpha S_0 & -\beta S_0 \\ 0 & -\theta & \alpha S_0 & \beta S_0 \\ 0 & \theta & -B_T & 0 \\ 0 & 0 & \tau - \varepsilon\tau & -\psi_2 \eta \end{bmatrix}, \tag{13}$$

where

$$B_T = \gamma + \psi_1 + \tau. \tag{14}$$

One of the eigenvalues is $-c_m$. The other three are eigenvalues of the matrix

$$\begin{bmatrix} -\theta & \alpha S_0 & \beta S_0 \\ \theta & -B_T & 0 \\ 0 & \tau - \varepsilon\tau & -\psi_2 \eta \end{bmatrix}, \tag{15}$$

whose characteristic equation is

$$a_3 x^3 + a_2 x^2 + a_1 x + a_0 = 0, \tag{16}$$

where

$$a_0 = \psi_2 \eta B_T \theta - \alpha S_0 \psi_2 \eta \theta - \beta \theta S_0 (1-\varepsilon)\tau, \tag{17}$$

$$a_1 = \theta \psi_2 \eta + \psi_2 \eta B_T + B_T \theta - \alpha S_0 \theta, \tag{18}$$

$$a_2 = \theta + B_T + \psi_2 \eta, \tag{19}$$

$$a_3 = 1. \tag{20}$$

The Routh-Hurwitz stability criteria for a 3×3 matrix is that all values of the determinant of Hurwitz matrices are positive. The determinants of Hurwitz matrices are:

$$D_1 = |a_2| > 0, \tag{21}$$

where $a_2 > 0$ and

$$D_2 = \begin{bmatrix} a_2 & a_0 \\ 1 & a_1 \end{bmatrix} > 0. \tag{22}$$

From (22), we have $a_1 a_2 - a_0 > 0$ or $a_1 a_2 > a_0$

$$D_3 = \begin{bmatrix} a_2 & a_0 & 0 \\ 1 & a_1 & 0 \\ 0 & a_2 & a_0 \end{bmatrix}. \tag{23}$$

(23) gives $a_0(a_1 a_2 - a_0) > 0$.

Clearly, a_2 is positive in (19). Also, $a_1 a_2 > a_0$ or $a_1 a_2 - a_0 > 0$, in (17), (18), and (19). Finally, we shall show that a_0

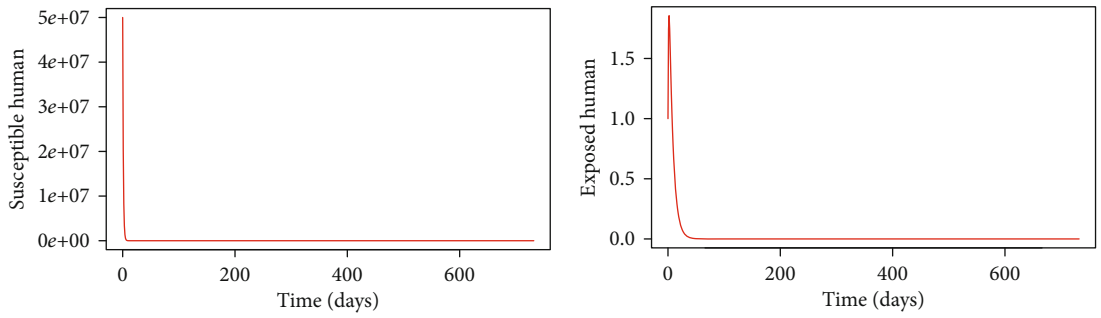

Figure 1: Time series solution of susceptible and exposed population of COVID-19.

$(a_1a_2 - a_0) > 0$. Since $a_1a_2 - a_0$ is positive, then, we need to show that a_0 is also positive so that $a_0(a_1a_2 - a_0) > 0$.

$$a_0 = \psi_2\eta B_T\theta - (\alpha S_0\psi_2\eta\theta + \beta\theta S_0(1-\varepsilon)\tau) > 0,$$
$$1 - \frac{\alpha S_0\psi_2\eta\theta + \beta\theta S_0(1-\varepsilon)\tau}{\psi_2\eta B_T\theta} > 0, \quad (24)$$
$$1 - R_c > 0.$$

Hence, $1 - R_c > 0$ if $R_c < 1$. Therefore, $a_0 > 0$ if $R_c < 1$. Hence, by Routh-Hurwitz theorem [22], all the eigenvalues of the Jacobian matrix J_{E_0} have negative real parts when $R_c < 1$ and the disease-free equilibrium solution is locally asymptotically stable if $R_c < 1$. The following theorem summarizes the above result in what follows:

Theorem 2. *The disease-free equilibrium solution is locally asymptotically stable if $R_c < 1$.*

Remark 3. The biological meaning of the theorem above is that COVID-19 eradication depends on the initial number of the infectious individuals in the population. This implies that a small invasion of infectious individuals into a completely susceptible population will not lead to an outbreak of the disease.

We present in Figures 1, 2, 3, and 4 the time series solution of the susceptible, exposed, infected, and partially recovered population of COVID-19, the prevalence against time for the unforced COVID-19 model with associated wavelet spectrum, and the estimated wavelet spectrum of the first week of the year 2 and year 4.5 for the unforced COVID-19 model.

3.2. Global Stability of Disease-Free Equilibrium Solution. The global asymptotic stability of models (19), (20), (22), and (23) is explored in what follows.

Theorem 4. *The disease-free equilibrium E_0 is globally asymptotically stable if $R_c \leq 1$ and unstable if $R_C > 1$.*

Proof. Consider the Lyapunov function.

$$L = \psi_2\eta I_H + \left(S_0\beta + \frac{S_0\alpha\psi_2\eta}{(1-\varepsilon)\tau}\right)P_C. \quad (25)$$

Its time derivative is

$$L' = \psi_2\eta\frac{dI_H}{dt} + \left(S_0\beta + \frac{S_0\alpha\psi_2\eta}{(1-\varepsilon)\tau}\right)\frac{dP_C}{dt},$$
$$L' = \psi_2\eta(\theta E_H - B_T I_H) + \left(S_0\beta + \frac{S_0\alpha\psi_2\eta}{(1-\varepsilon)\tau}\right) \cdot ((1-\varepsilon)\tau I_H - \psi_2\eta P_C),$$
$$L' = S_0\alpha\psi_2\eta I_H + S_0\beta(1-\varepsilon)\tau I_H - \psi_2\eta B_T I_H + \psi_2\eta\theta E_H - S_0\beta\psi_2\eta P_C - \frac{S_0\alpha\psi_2^2\eta^2 P_C}{(1-\varepsilon)\tau},$$
$$= \psi_2\eta B_T I_H\left(\frac{\alpha S_0\psi_2\eta + \beta S_0(1-\varepsilon)\tau}{\psi_2\eta B_T} - 1\right) + \psi_2\eta\left(\theta E_H - S_0\beta P_C - \frac{S_0\alpha\psi_2\eta P_C}{(1-\varepsilon)\tau}\right),$$
$$= \psi_2\eta B_T I_H(R_c - 1) - \psi_2\eta\left(\frac{S_0\alpha\psi_2\eta P_C}{(1-\varepsilon)\tau} + S_0\beta P_C - \theta E_H\right)$$
$$\leq \psi_2\eta B_T I_H(R_c - 1), \leq 0 \text{ if } R_c \leq 1. \quad (26)$$

Therefore, $L' \leq 0$ if $R_C \leq 1$ with $L' = 0$ if and only if $R_c = 1$ or $E_H = I_H = P_C = 0$. It follows that the largest invariant subset in $\{(S_H, E_H, I_H, P_C) \in T : L' = 0\}$ is the singleton E_0, and hence by LaSalle's invariance principle [23], the disease-free equilibrium E_0 will be approached by all solution trajectories, and hence, the disease-free equilibrium solution is globally asymptotically stable.

Remark 5. The epidemiological implication of the above theorem is that COVID-19 can be eradicated irrespective of the initial sizes of the subpopulation of the model.

3.3. Global Stability of the Endemic Equilibrium Point. The endemic equilibrium solution $E_1 = (S_H^*, E_H^*, I_H^*, P_C^*)$ satisfies the following equations:

$$\lambda_h - \alpha S_H^* I_H^* - \beta S_H^* P_C^* - c_m S_H^* = 0, \quad (27)$$

$$\alpha S_H^* I_H^* + \beta S_H^* P_C^* - \theta E_H^* = 0, \quad (28)$$

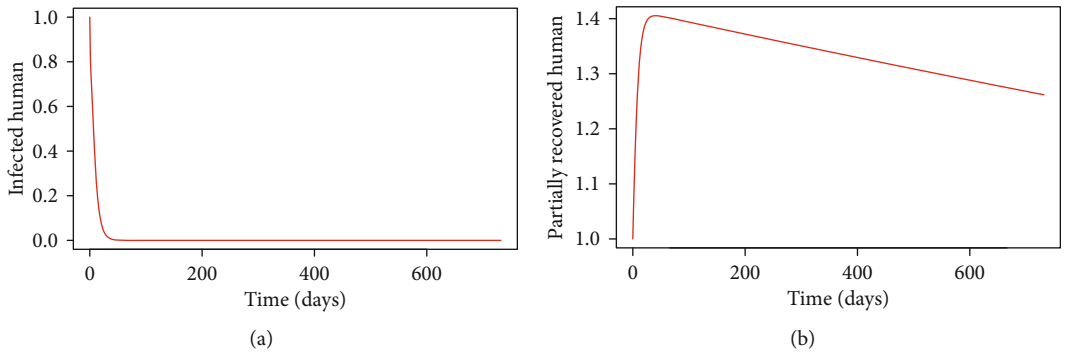

Figure 2: Time series solution of infected and partially recovered population of COVID-19.

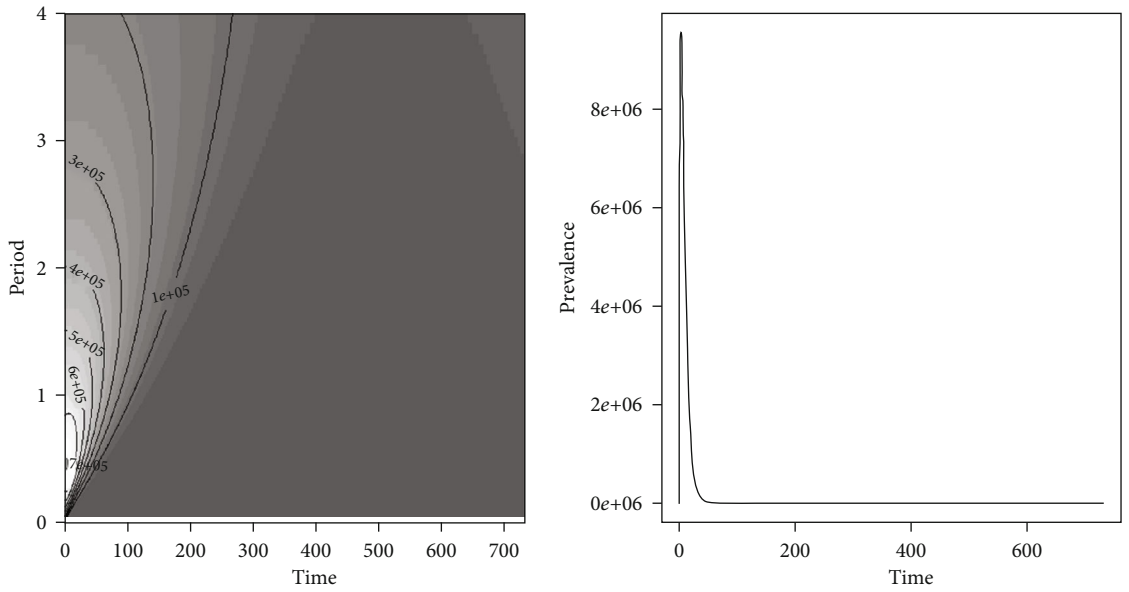

Figure 3: Prevalence against time for the unforced COVID-19 model with associated wavelet spectrum.

$$\theta E_H^* - B_T I_H^* = 0, \tag{29}$$

$$(1-\varepsilon)\tau I_H^* - \psi_2 \eta P_C^* = 0. \tag{30}$$

Finding S_H^*, I_H^*, and P_C^* in (27), (28), (29), and (30) gives

$$S_H^* = \frac{\lambda_h}{\alpha I_H^* + \beta P_C^* + c_m}, \tag{31}$$

$$I_H^* = \frac{\theta E_H^*}{B_T}, \tag{32}$$

$$P_C^* = \frac{(1-\varepsilon)\tau I_H^*}{\psi_2 \eta}. \tag{33}$$

Adding (27) and (28), we get

$$\lambda_h - c_m S_H^* - \theta E_H^* = 0. \tag{34}$$

Substituting (31) and (32) in (33) into (34) gives the following

$$-\frac{\theta c_m R_c (E_H^*)^2}{\lambda_h} + c_m (R_C - 1) E_H^* = 0. \tag{35}$$

From (35), we can obtain E_H^* to be

$$E_H^* = \frac{\lambda_h}{\theta}\left(1 - \frac{1}{R_C}\right). \tag{36}$$

Substituting E_H^* in (31), (32), and (33) gives

$$\begin{aligned} S_H^* &= \frac{\lambda_h}{c_m R_C}, \\ I_H^* &= \frac{\lambda_h}{B_T}\left(1 - \frac{1}{R_C}\right), \\ P_C^* &= \frac{(1-\varepsilon)\tau\lambda_h}{B_T \psi_2 \eta}\left(1 - \frac{1}{R_C}\right). \end{aligned} \tag{37}$$

Thus, the endemic equilibrium solution exists whenever $R_c > 1$.

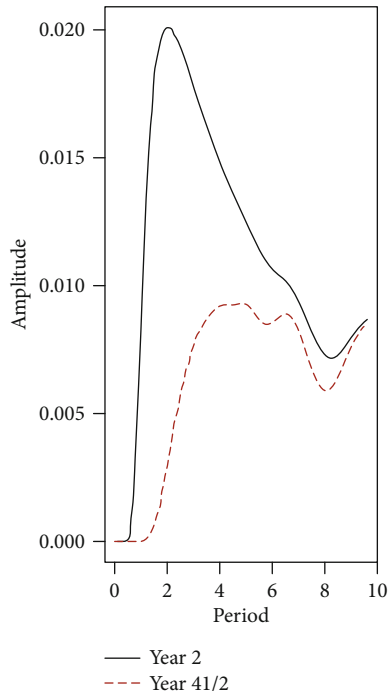

FIGURE 4: The estimated wavelet spectrum at the first week of year 2 and year 4.5 for the unforced COVID-19 model.

Furthermore, we establish the global asymptotic stability of the endemic equilibrium solutions converging to the endemic equilibrium point for $R_c > 1$. We shall carry out this, by constructing a suitable Lyapunov function of Goh-Volterra type; see [24]. The result below establishes the global stability of the endemic equilibrium solution E_1.

Theorem 6. *The unique endemic equilibrium E_1 is globally asymptotically stable whenever $R_c > 1$.*

Proof. Given the following equations which are satisfied by the endemic equilibrium point E_1,

$$\lambda_h = (\alpha I_H^* + \beta P_C^*)S_H^* + c_m S_H^*, \tag{38}$$

$$(\alpha I_H^* + \beta P_C^*)S_H^* = \theta E_H^*, \tag{39}$$

$$\theta E_H^* = B_T I_H^*, \tag{40}$$

$$(1-\varepsilon)\tau = \psi_2 \gamma P_C^*. \tag{41}$$

Consider the following Goh-Volterra Lyapunov function

$$V = \left(S_H - S_H^* - S_H^* \ln \frac{S_H}{S_H^*}\right) + \left(E_H - E_H^* - E_H^* \ln \frac{E_H}{E_H^*}\right) + a\left(I_H - I_H^* - I_H^* \ln \frac{I_H}{I_H^*}\right) + b\left(P_C - P_C^* - P_C^* \ln \frac{P_C}{P_C^*}\right), \tag{42}$$

where $a = \alpha S_H^*/B_T$ and $b = \beta S_H^*/\psi_2\gamma$, with the Lyapunov time derivative obtained as

$$\begin{aligned} V' &= \left(1 - \frac{S_H^*}{S_H}\right)S_H' + \left(1 - \frac{E_H^*}{E_H}\right)E_H' \\ &\quad + a\left(1 - \frac{I_H^*}{I_H}\right)I_H' + b\left(1 - \frac{P_C^*}{P_C}\right)P_C', \\ V' &= \left(1 - \frac{S_H^*}{S_H}\right)(\lambda_h - (\alpha I_H + \beta P_C)S_H - c_m S_H \\ &\quad + \left(1 - \frac{E_H^*}{E_H}\right)((\alpha I_H + \beta P_C)S_H - \theta E_H) \\ &\quad + a\left(1 - \frac{I_H^*}{I_H}\right)(\theta E_H - B_T I_H) \\ &\quad + b\left(1 - \frac{P_C^*}{P_C}\right)(1-\varepsilon)\tau I_H - \psi_2 \gamma P_C\Big). \end{aligned} \tag{43}$$

Using (38), we have

$$\begin{aligned} V' &= \left(1 - \frac{S_H^*}{S_H}\right)(\alpha I_H^* + \beta P_C^*)S_H^* + c_m S_H^* - (\alpha I_H + \beta P_C)S_H \\ &\quad - c_m S_H + \left(1 - \frac{E_H^*}{E_H}\right)((\alpha I_H + \beta P_C)S_H - \theta E_H) \\ &\quad + a\left(1 - \frac{I_H^*}{I_H}\right)(\theta E_H - B_T I_H) + b\left(1 - \frac{P_C^*}{P_C}\right) \\ &\quad \cdot ((1-\varepsilon)\tau I_H - \psi_2 \gamma P_C). \end{aligned} \tag{44}$$

Further simplification gives

$$\begin{aligned} V' &= (\alpha I_H^* + \beta P^* C)S_H^* + \theta E_H^* + a B_T I_H^* + b\psi_2 \gamma P_C \\ &\quad - (\alpha S_H^* + \beta P_C^*)\frac{(S_H^*)^2}{S_H} - (\alpha I_H + \beta P_C)\frac{S_H E_H^*}{E_H} \\ &\quad - \frac{a\theta E_H I_H^*}{I_H} - \frac{b(1-\varepsilon)\tau I_H P_C^*}{P_C} + 2c_m S_H^* \\ &\quad - \frac{c_m (S_H^*)^2}{S_H} - c_m S_H + (\alpha I_H + \beta P_C)S_H^* - \theta E_H \\ &\quad + a\theta E_H - a B_T I_H + b(1-\varepsilon)\tau I_H - b\psi_2 \gamma P_C. \end{aligned} \tag{45}$$

Replacing a and b by their values and exploiting (38), (39), (40), and (41) give

$$a\theta = \frac{\alpha S_H^* I_H^*}{E_H^*}, \tag{46}$$

$$d(1-\varepsilon)\tau = \frac{\beta S_H^* P_C^*}{I_H^*}. \tag{47}$$

Using (38), (39), (40), (41), (46), and (47), we have

$$\begin{aligned} V' &= c_m S_H^* \left(2 - \frac{S_H^*}{S_H} - \frac{S_H}{S_H^*}\right) + 3\alpha S_H^* I_H^* - \alpha I_H^* \frac{(S_H^*)^2}{S_H} \\ &\quad - \alpha S_H I_H \frac{E_H^*}{E_H} - \frac{\alpha S_H^* E_H (I_H^*)^2}{E_H^* I_H} + 3\beta S_H^* P_C^* \\ &\quad - \beta P_C^* \frac{(S_H^*)^2}{S_H} - \frac{\beta P_C S_H E_H^*}{E_H} - \frac{\beta S_H^* I_H (P_C^*)^2}{I_H^* P_C}, \\ V' &= c_m S_H^* \left(2 - \frac{S_H^*}{S_H} - \frac{S_H}{S_H^*}\right) + \alpha S_H^* I_H^* \\ &\quad \cdot \left(3 - \frac{S_H^*}{S_H} - \frac{S_H E_H^* I_H}{S_H^* E_H I_H^*} - \frac{E_H I_H^*}{E_H^* I_H}\right) + \beta S_H^* P_C^* \\ &\quad \cdot \left(3 - \frac{S_H^*}{S_H} - \frac{S_H E_H^* P_C}{S_H^* E_H P_C^*} - \frac{I_H P_C^*}{I_H^* P_C}\right). \end{aligned} \tag{48}$$

Using arithmetic-geometric means inequality, i.e., $n - (a_1 + a_2 + \cdots + a_n) \leq 0$, where $a_1.a_2 \cdots a_n = 1$ and $a_1, a_2, \cdots, a_n > 0$, it follows that $V' \leq 0$ with $V = 0$ if and only if $S_H = S_H^*$, $E_H = E_H^*$, $I_H = I_H^*$, and $P_C = P_C^*$.

Hence, the largest compact invariant subset of the set where $V' = 0$ is $(S_H, E_H, I_H, P_C) = (S_H^*, E_H^*, I_H^*, P_C^*)$ and by classical stability theorem of Lyapunov and LaSalle's Invariance Principle, it follows that every solution in T approaches E_1 for $R_c > 1$ as $t \to \infty$.

Remark 7. The epidemiological implication of the above result is that COVID-19 will establish itself whenever $R_c > 1$ in the population.

4. Uncertainty and Sensitivity Analysis

4.1. Local Sensitivity Analysis. In this section, we carried out sensitivity analysis of parameters of model systems (7), (8), (9), and (10) in order to determine the relative importance of the model parameters on the disease infection. To determine how best to reduce the infection, it is necessary to know the relative importance of the different factors responsible for the infections.

Sensitivity indices could be computed numerically so as to figure out parameters that have high impact on basic reproduction number R_c and which of the parameters should be given preferential treatment by intervention strategies.

Analytically, sensitivity analysis on all parameters which account for disease dynamics is done using the Chitnis et al. [25] approach; we compute sensitivity indices of the R_c which measures initial disease infection and allows us to measure the relative change in a state variable when a variable changes.

The normalized forward sensitivity index of a variable to a parameter is the ratio of the relative change in the variable to the relative change in the parameter. When the variable is a differentiable function of the parameter, the sensitivity index may be alternatively defined using partial derivatives.

Definition. The normalized forward sensitivity index of a variable, u, that depends differentially on a parameter, p, is defined as

$$N_p^u = \frac{\partial u}{\partial p} \times \frac{p}{u}, \tag{49}$$

for $u \neq 0$.

Consequently, we derive analytical expression for the sensitivity index of R_C as

$$N_{p_i}^{R_c} = \frac{\partial R_c}{\partial p_i} \times \frac{p_i}{R_c}, \tag{50}$$

where $p_i, i \in \mathbb{N}$ denotes each parameter involved in R_c.

Using

$$R_c = \frac{\alpha S_0 \psi_2 \eta + \beta S_0 (1 - \varepsilon)\tau}{\psi_2 \eta B_T}, \tag{51}$$

where $S_0 = \lambda_h / c_m$.

$$B_T = \gamma + \psi_1 + \tau. \tag{52}$$

We compute the sensitivity index of each parameter with respect to the R_C, for instance

$$N_\alpha^{R_c} = \frac{\partial R_c}{\partial \alpha} \times \frac{\alpha}{R_c} = 0.999. \tag{53}$$

We have Table 1 which summarizes the sensitivity indices of R_c with respect to parameters

$$N_{\lambda_h}^{R_c}, N_{c_m}^{R_c}, N_\gamma^{R_c}, N_{\psi_1}^{R_c}, N_\beta^{R_c}, N_\varepsilon^{R_c}, N_{\psi_2}^{R_c}, N_\tau^{R_c}. \tag{54}$$

4.1.1. Interpretation of Sensitivity Indices Obtained in Table 2. The computed sensitivity indices on R_c with respect to the involved parameters give insights to the model system proposed. Provided all parameters remain constant, most sensitive parameters are α, λ_h (the contact rate between susceptible and infectious individuals, natural birth rate). The implication is that the increase in contact rate between susceptible and infectious individuals and natural birth rate have high tendency to increase in COVID-19 epidemic due to positive variation on basic reproduction number R_c. γ (COVID-19-induced rate) is the only parameter that has no effect on the spread of the disease. Interestingly, improvement in slower rate of recovery (η) and increase in transition rate from the infectious disease class to the partially recovered (τ) one are major parameters that reduce the disease epidemic. In the same vein, the sensitivity indexes of c_m, ψ_1, ψ_2 reveal that the increase in containment rate of susceptible individuals, recovery rate of infectious individuals, and recovery rate of partially recovered carriers contribute to the reduction in the spread of COVID-19 infection.

In light of this, we recommend that the World health Organization (WHO) should put in place health interventions and strategies that will not only improve the slower

Table 1: Summary of the parameters.

Parameter	Meaning	Value	Reference
α	Contact rate between susceptible and infectious individuals	0.75	Assumed
β	Contact rate between susceptible and partially recovered individuals	0.75	Assumed
θ	Transition rate from exposed to infectious class	0.143	[15]
ψ_1	Recovery rate of infectious individuals	0.33029	[15]
γ	COVID-19-induced death rate	1.7826×10^{-5}	[15]
ψ_2	Recovery rate of partially recovered carriers	[0.000315] $(\text{day})^{-1}$	Assumed
τ	Transition rate from infectious class to partially recovered	0.1	Assumed
ε	Proportion of the infectious individuals who recover fully	0.5	Assumed
ϕ	Loss of immunity rate	0.0017	Assumed
η	Slower rate of recovery	0.5[0-1]	Varied
c_m	Containment rate of susceptible individuals	Variable (0-1)	Assumed
λ_h	Natural birth rate	600	Assumed

Containment rate of susceptible individuals (c_m).

Table 2: Numerical values of sensitivity indices of R_c with respect to the parameter involved.

Parameter symbol	Sensitivity index
α	+0.999
λ_h	+1.000
c_m	−1.00
γ	0.00
ψ_1	−0.16
β	0.049
ε	0.049
η	−11709.42
ψ_2	−0.46
τ	−4652.26

recovery rate of the partially recovered individuals but also increase the transition rate from the infectious class to partially recovered one.

4.2. Global Sensitivity Analysis. The global sensitivity analysis helps to investigate the change in the output values resulting from changes in all parameter values over the ranges in parameters ([26]. To perform the global sensitivity analysis of the reproduction number R_c and the range of values in Table 3. We aim here to establish the most influential parameters in R_c and also give some insightful ideas from the PRCC plot by running a sample size of 1,000. It was observed that the scatter plot in Figures 5–8 shows a positive relation between R_c and parameters α,β, θ, ψ_1, ψ_2, τ, ϕ, η, λ_h, ε, and γ have a negative relation between them and R_c. We understand that the positive relation here implies that a high rate of either of these parameters α,β, θ, ψ_1, ψ_2, τ, ϕ, and η will generate a higher transmission rate during an outbreak, while the negative relation for λ_h, ε, and γ will aid in decreasing the severity of the disease-induced death rate. Figure 8(a) presents well defined simulation results of the scatter plots in Figures 5–8 and that of the numerical signs in Table 2. Figure 8(a) also indicates that the most influential parameters that can make the disease spread fast are α,θ, ψ_1, and τ. Here, any effort to reduce the relative relevance or impact of α, θ, ψ_1, and τ will reduce the spreading rate of COVID-19. Figure 9(b) shows that while R_c (reproduction number) is decreasing with an increase in β, it increases with an increase in ψ_2.

5. Analysis of Optimal Control Strategies against COVID-19

There are several measures of prevention and control of infectious diseases, but in this paper, we employ the nonpharmaceutical intervention (NPI), like social distancing, u_1 , and the nonspecific treatment effort, u_2.

5.1. Social Distancing $u_1(t)$. This is a nonpharmaceutical intervention (NPI), also known as physical distancing, which refers to the measures taken to prevent the spread of COVID-19 disease by maintaining a specific physical distance between individuals and reducing the number of time persons come in close contact with one another.

5.2. Treatment $u_2(t)$. This involves the use of an agent, procedure, or regimen, such as a drug to cure or mitigate the COVID-19 disease. This treatment employed here is a nonspecific regimen.

Here, we introduce these time-dependent interventions $(u_1(t), u_2(t))$ where $u_1(t)$ is the time-dependent preventive effort which we refer to as *social distancing*, while $u_2(t)$ is the time-dependent treatment effort which is an unspecific regimen to slow the spread of COVID-19. These two control functions are expected to be bounded and Lebesgue integrable on the closed interval $[0, T]$, where T is the

Table 3: Model parameter descriptions and range.

Parameter	Meaning	Range
α	Contact rate between susceptible and infectious individuals	0.75–1.5
β	Contact rate between susceptible individuals and partially recovered ones	0.75–1.5
θ	Transition rate from the exposed to infectious class	0.143–1.0
ψ_1	Recovery rate of infectious individuals	0.33029–0.5
γ	COVID-19-induced death rate	0.000017826–0.0010982
ψ_2	Recovery rate of partially recovered carriers	0.000315–0.04398
τ	Transition rate from the infectious class to the partially recovered one	0.1–0.2384
ε	Proportion of the infectious individuals who recover fully	0.5–1.0
ϕ	Loss of immunity rate	0.0017–1.0
c_m	Containment rate of susceptible individuals	(0–1)
λ_h	Natural birth rate of human	0.038–0.5
ν	Slower rate of recovery	0.5–1.5

duration of time for which we apply our control measures. The COVID-19 models (1), (2), (3), (4), (5), and (7) become

$$\frac{dS_H}{dt} = \lambda_h - \alpha(1-u_1(t))S_H I_H - \beta(1-u_1(t))S_H P_C - c_m S_H, \tag{55}$$

$$\frac{dE_H}{dt} = \alpha(1-u_1(t))S_H I_H + \beta(1-u_1(t))S_H P_C - \theta E_H, \tag{56}$$

$$\frac{dI_H}{dt} = \theta E_H - \gamma I_H - \psi_1 I_H - \tau I_H - u_2(t) I_H, \tag{57}$$

$$\frac{dP_C}{dt} = (1-\varepsilon)\tau I_H - \psi_2 \eta P_C, \tag{58}$$

$$\frac{dR_H}{dt} = \varepsilon\tau I_H + \psi_1 I_H + \psi_2 \eta P_C + u_2(t) I_H, \tag{59}$$

with initial conditions

$$\begin{aligned} S_H(0) &= S_h^0 > 0, \\ E_H(0) &= E_H^0, \\ I_H(0) &= I_H^0(0) > 0, \\ P_C(0) &= P_C^0(0), \\ R_H(0) &= R_H^0(0) > 0. \end{aligned} \tag{60}$$

The model equation can be written in the vectorial form

$$\frac{dS_H}{dt} = g_1(S_H(t), E_H(t), I_H(t), P_C(t), R_H(t)), \tag{61}$$

$$\frac{dE_H}{dt} = g_2(S_H(t), E_H(t), I_H(t), P_C(t), R_H(t)), \tag{62}$$

$$\frac{dI_H}{dt} = g_3(S_H(t), E_H(t), I_H(t), P_C(t), R_H(t)), \tag{63}$$

$$\frac{dP_C}{dt} = g_4(S_H(t), E_H(t), I_H(t), P_C(t), R_H(t)), \tag{64}$$

$$\frac{dR_H}{dt} = g_5(S_H(t), E_H(t), I_H(t), P_C(t), R_H(t)). \tag{65}$$

$N_H(0) = N_{H,0} > 0$, for $N_H = (S_H(t), E_H(t), I_H(t), P_C(t), R_H(t))$. $dN_H/dt = \Lambda_h - c_m S_H - \gamma I_H \le \Lambda_h - c_m N_H - \gamma N_H$ where the model parameters are nonnegative. The goal here is to determine the optimal control strategy which minimizes the number of symptomatic infectious humans and the cost of the control measures and to predict the impact of these control measures as a means to advice public health officials on the best control and/or elimination policies. The control functions $u_1(t)$ and $u_2(t)$ are defined on the closed interval $[0, T]$, where $0 \le u_1(t) \le 1$ and $0 \le u_2(t) \le 1$. The objective functional is defined mathematically which is given by

$$J(u_1(t), u_2(t)) = \int_0^T \left(\omega I_H + \frac{c_1}{2}u_1^2 + \frac{c_2}{2}u_2^2\right) dt, \tag{66}$$

where ω, c_1, and c_2 denote the weight constants (it is a parameter which describes the comparative importance of the two terms in the functional) for the relative costs of I_H and the control interventions. Hence, there is need to obtain an optimal control pair $(u_1^*(t), u_2^*(t))$ such that

$$J(u_1^*(t), u_2^*(t)) = \min_{u_1, u_2 \in \Omega} J(u_1(t), u_2(t)), \tag{67}$$

where $\Omega = \{(u_1(t), u_2(t)) \mid 0 \le u_1(t) \le 1, 0 \le u_2(t) \le 1\}$.

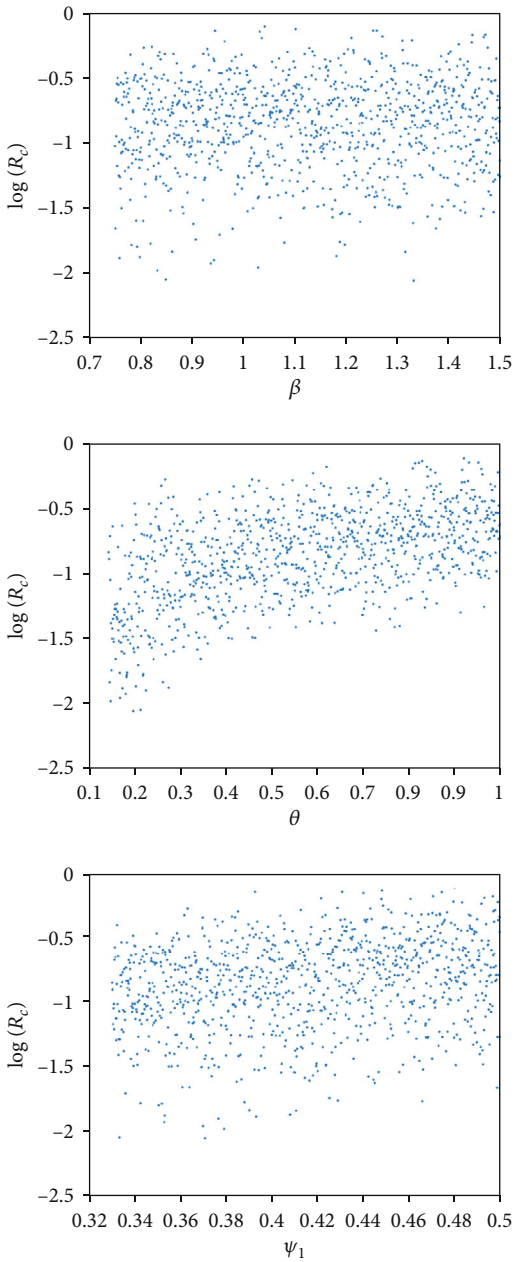

Figure 5: The scatter diagrams for some selected parameters in R_C (scatter plots of β, θ, and ψ_1, in R_C).

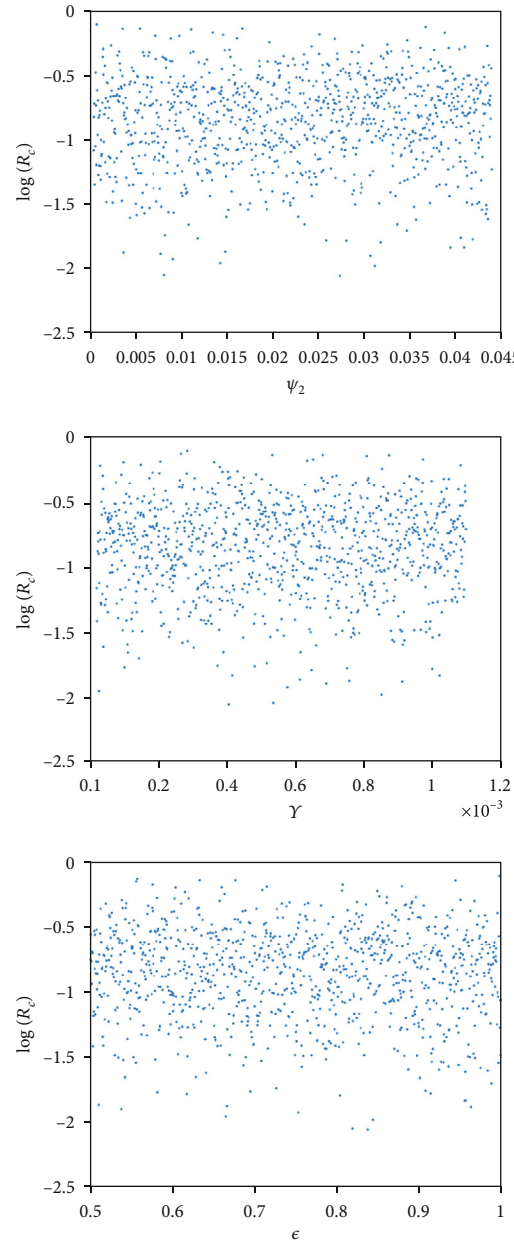

Figure 6: The scatter diagrams for some selected parameters in R_C (scatter plots of ψ_2, γ, and ε in R_C).

5.3. The Optimal Control Problem Statement. Here, we present the optimal control problem for the COVID-19 disease which is stated as follows:

$$J(u_1(t), u_2(t)) = \int_0^T \left(\omega I_H + \frac{c_1}{2}u_1^2 + \frac{c_2}{2}u_2^2\right)dt, \tag{68}$$

subject to the dynamics

$$\frac{dS_H}{dt} = \lambda_h - \alpha(1-u_1(t))S_H I_H - \beta(1-u_1(t))S_H P_C - c_m S_H, \tag{69}$$

$$\frac{dE_H}{dt} = \alpha(1-u_1(t))S_H I_H + \beta(1-u_1(t))S_H P_C - \theta E_H, \tag{70}$$

$$\frac{dI_H}{dt} = \theta E_H - \gamma I_H - \psi_1 I_H - \tau I_H - u_2(t) I_H, \tag{71}$$

$$\frac{dP_C}{dt} = (1-\varepsilon)\tau I_H - \psi_2 \eta P_C, \tag{72}$$

$$\frac{dR_H}{dt} = \varepsilon\tau I_H + \psi_1 I_H + \psi_2 \eta P_C + u_2(t) I_H, \tag{73}$$

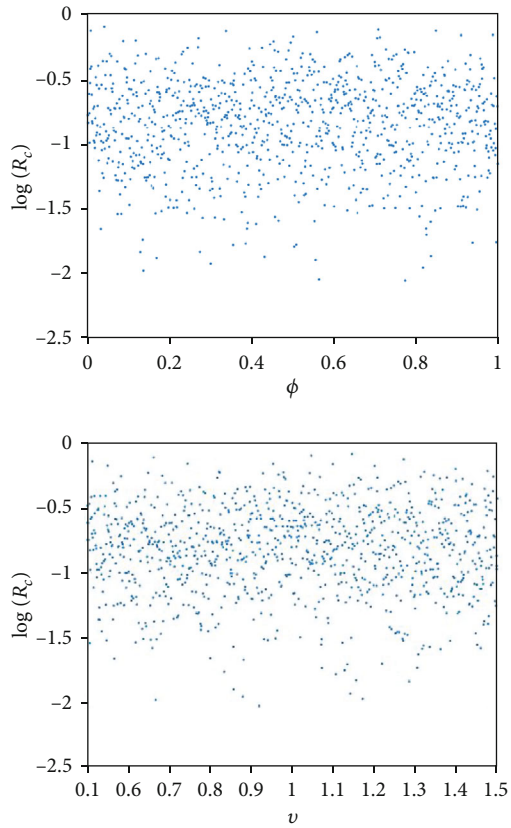

FIGURE 7: The scatter diagrams for some selected parameters in R_C (scatter plots of ϕ and υ in R_C).

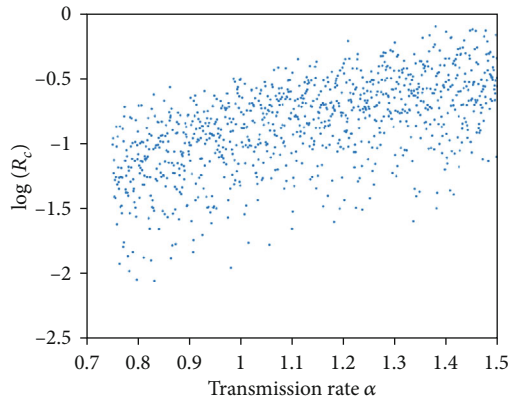

FIGURE 8: The scatter diagrams for some selected parameters in R_C (scatter plots of α in R_C).

with initial conditions

$$\begin{aligned} S_H(0) &= S_h^0 > 0, \\ E_H(0) &= E_H^0, \\ I_H(0) &= I_H^0(0) > 0, \\ P_C(0) &= P_C^0(0), \\ R_H(0) &= R_H^0(0) > 0. \end{aligned} \tag{74}$$

The terminal or final time T is fixed and subjected to the control constraints.

$$\begin{aligned} &u_1, u_2 \in \Omega, \\ &\forall t \in [0, T]. \end{aligned} \tag{75}$$

There is a need to solve the following optimal control problem such that we find a control $u_1^*(t), u_2^*(t)$ which minimizes the objective functional, that is

$$J(u_1^*(t), u_2^*) = \min_{u_1, u_2 \in \Omega} J(u_1(t), u_2(t)). \tag{76}$$

If there exist such $u_1(t), u_2(t)$, it is referred to as optimal control. The optimal control along side with the corresponding solution gives the optimal control pair

$$(S_H^*(t), E_H^*(t), I_H^*(t), P_C^*(t), R_H^*(t), u_1^*(t), u_2^*(t)). \tag{77}$$

The first question that we must address is to confirm whether an optimal control pair $(S_H^*(t), E_H^*(t), I_H^*(t), P_C^*(t), R_H^*(t), u_1^*(t), u_2^*(t))$ exists. Thus, this question of existence is settled by the following Lemma.

Lemma 8. *(Filippov-Cesari existence theorem). For all* $(t, x) \in \mathbb{R}^{n+1}$*, define the set*

$$L(t, x) = \{(f(x, u) + \zeta, g(x, u)) : \zeta \leq 0, u \in U\}. \tag{78}$$

Suppose that

(1) $L(t, x)$ *is convex for every* (t, x)

(2) U *is compact*

(3) There exists a constant $M > 0$ *such that* $\|x(t)\| \leq M$ *for all* $t \in [0, T]$ *and all admissible pairs* (x, u)

Then, $\exists$ *is an optimal pair* $(x^*(t), u^*(t))$ *where* $u^*(t) \in \Omega$.

Lemma 9. *Suppose that there exists a solution of the optimal control problem (68)–(75).*

Proof. We rewrite systems (68)–(73) as follows

$$\begin{aligned} \frac{d}{dt}\begin{pmatrix} S_H \\ E_H \\ I_H \\ P_c \\ R_H \end{pmatrix} &= \begin{pmatrix} g_1(S_H(t), E_H(t), I_H(t), P_C(t), R_H(t)) \\ g_2(S_H(t), E_H(t), I_H(t), P_C(t), R_H(t)) \\ g_3(S_H(t), E_H(t), I_H(t), P_C(t), R_H(t)) \\ g_4(S_H(t), E_H(t), I_H(t), P_C(t), R_H(t)) \\ g_5(S_H(t), E_H(t), I_H(t), P_C(t), R_H(t)) \end{pmatrix} \\ &= g(S_H(t), E_H(t), I_H(t), P_C(t), R_H(t)), \end{aligned} \tag{79}$$

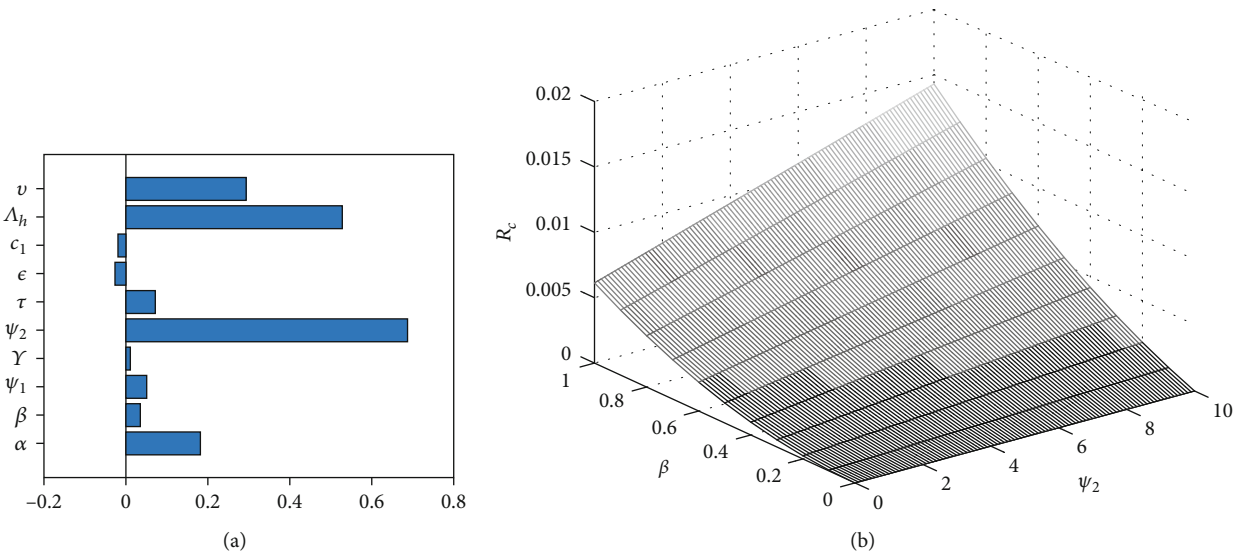

FIGURE 9: Partial rank correlation coefficient (PRCC) of the parameters in R_C (Tornado plot of parameters in R_c) in Figure 9(a). The coupling effects of both the recovery rate of partially recovered carriers and the contact rate between susceptible individuals and partially recovered ones on R_c (3D plot of ψ_2, β, and R_c)in Figure 9(b).

where $N_H = (S_H(t), E_H(t), I_H(t), P_C(t), R_H(t))$. We also define a set $V(t,N) = \{(f(N,u_i,t) + h_i g(N,u_i,t)): h > 0, u_i \in U\}$ according to the Filippov-Cesari theorem [27], [26].

Here, we first show that $V(t,N)$ is a convex for (t,N).

Suppose that $z_1, z_2 \in V(t,N)$, we show that $V(t,N)$ is a convex for each (t,N) by proving that the line connecting z_1 and z_2 is completely in $V(t,N)$. Thus, we need show that $\rho z_{i1} + (1-\rho)z_2 \in V(t,N) \forall \rho \in [0,1]$. For $x_i \in V(t,N) \Rightarrow \exists h_1, h_2 \le 0$ and that the control function $u_1(t), u_1(t) \in U$ such that $z_i = \{(f(N,u_i,t) + h_i g(N,u_i,t)): h > 0, u_i \in U\}$ for $i = 1,2$. Let $f(N,u_i,t) = \omega I_H + (1/2)c_i u_i^2$, $i = 1,2$,and $g(N,u_i,t) = RHS\ of\ 69-73$.

Thus, we have

$$\begin{aligned}
&\rho(f(N,u_1,u_2,t) + h_1) + (1-\rho)(f(N,u_3,u_4,t) + h_2)\\
&\quad = \rho\left(\omega I_H + \frac{1}{2}c_1 u_1^2 + \frac{1}{2}c_2 u_2^2\right)\\
&\qquad + (1-\rho)\left(\omega I_H + \frac{1}{2}c_1 u_3^2 + \frac{1}{2}c_2 u_4^2\right) + \rho h_1 + (1-\rho)h_2\\
&\quad = \omega I_H + \rho\left(\frac{1}{2}c_1 u_1^2 + \frac{1}{2}c_2 u_2^2\right) + (1-\rho)\frac{1}{2}c_1 u_3^2 + \frac{1}{2}c_2 u_4^2\\
&\qquad + \rho h_1 + (1-\rho)h_2.
\end{aligned} \tag{80}$$

Suppose that $u_5 = \sqrt{\rho(u_1^2 + u_2^2) + (1-\rho)(u_3^2 + u_4^2)}$, it is observed that $u_5 \in U$ and if we let $h_3 \le 0. Y =$ Therefore, the first part of the convex combination belongs to $V(t,N)$. The second component will be checked as follows:

$$\begin{aligned}
&\rho(g(N,u_1,u_2,t)) + (1-\rho)(g(N,u_3,u_4,t))\\
&\quad = \rho[(\lambda_h - \alpha(1-u_1(t))S_H I_H - \beta(1-u_1(t))S_H P_C + c_m S_H)\\
&\qquad + (\alpha(1-u_1(t))S_H I_H + \beta(1-u_1(t))S_H P_C - \theta E_H)\\
&\qquad + (\theta E_H - \gamma I_H - \psi_1 I_H - \tau I_H - u_2(t)I_H)\\
&\qquad + ((1-\varepsilon)\tau I_H - \psi_2 \eta P_C) + (\varepsilon\tau I_H + \psi_1 I_H + \psi_2 \eta P_C\\
&\qquad + u_2(t)I_H)] + (1-\rho)[(\lambda_h - \alpha(1-u_3(t))S_H I_H\\
&\qquad - \beta(1-u_3(t))S_H P_C = c_m S_H) + (\alpha(1-u_3(t))S_H I_H\\
&\qquad + \beta(1-u_3(t))S_H P_C - \theta E_H) + (\theta E_H - \gamma I_H - \psi_1 I_H\\
&\qquad - \tau I_H - u_4(t)I_H) + ((1-\varepsilon)\tau I_H - \psi_2 \eta P_C)\\
&\qquad + (\varepsilon\tau I_H + \psi_1 I_H + \psi_2 \nu P_C + u_4(t)I_H)] = \Lambda_h\\
&\qquad - (\rho\alpha(1-u_1(t))S_H I_H + (1-\rho)\alpha(1-u_3(t))S_H I_H\\
&\qquad - (\rho\beta(1-u_1(t))S_H P_C + (1-\rho)\beta(1-u_3(t))S_H P_C\\
&\qquad - c_m S_H) + -(\rho\alpha(1-u_1(t))S_H I_H\\
&\qquad + (1-\rho)\alpha(1-u_3(t))S_H I_H + (\rho\beta(1-u_1(t))S_H P_C\\
&\qquad + (1-\rho)\beta(1-u_3(t)) - c_m S_H) - \theta E_H + \theta E_H - \gamma I_H\\
&\qquad - \psi_1 I_H - \tau I_H - (\rho u_2(t) + (1-\rho)u_4(t))I_H\\
&\qquad + (1-\varepsilon)\tau I_H - \psi_2 \eta P_C + \varepsilon\tau I_H + \psi_1 I_H + \psi_2 \eta P_C\\
&\qquad + (\rho u_2(t) + (1-\rho)u_4(t))I_H).
\end{aligned} \tag{81}$$

Suppose that $u_6 = \rho(u_1 + u_3) + (1-\rho)(u_3 + u_4)$. It is observed that u_6 belongs to U. Hence, we say finally that the convex combination of $\rho z_1 + (1-\rho)z_2$ is in $V(t,N,u_1,u_2)$ and U is clearly compact. Secondly, we show that the solution of (69)–(73) is bounded.

For all initial conditions in $\Delta = \{(S_H(t), E_H(t), I_H(t), P_C(t), R_H(t)) \in \mathbb{R}^5 : S_H(t) + E_H(t) + I_H(t) + P_C(t) + R_H(t) \le 1$

}, the trajectory obtained from the initial condition remains in a bounded domain included in Δ.

The total population is given by $N_H = S_H(t) + E_H(t) + I_H(t) + P_C(t) + R_H(t)$ with the derivative $(dN_H/dt) = \Lambda_h N_H - \mu_h N_H - \gamma I_H$.

It is observed that

$$0 \le I_H(t) \le N_H(t),$$
$$\Lambda_h - c_m N_H - \gamma I_H \le \frac{dN_H}{dt} \le \Lambda_h N_H - c_m N_H - \gamma N_H,$$
$$\frac{dN_H}{dt} \le \Lambda_h N_H - \mu_h N_H - \gamma N_H. \tag{82}$$

We have that $N_H(t) \le \sup_t \bar{N}_H$ where N_H is the solution of equation

$$\frac{dN_H}{dt} \le \Lambda_h - c_m N_H - \gamma N_H. \tag{83}$$

Thus, $\sup_t N_H \le \max\{N_{H,0}, N_H\}$. If $N_{H,0} \le N_H$, then $\max_t\{N_H(t)\} \le N_H$. If any solution exists, we can find it with the Pontryagin's maximum principle (PMP). This is done first, by incorporating a time-varying Lagrange multiplier $\lambda(t)$, whose elements are referred to as the adjoint or costate variables. We hereby analyse the model equations (68), (69), (70), (71), (72), (73), and (75) with control variables $(u_1(t), u_2(t))$. We seek an optimal control $(u_1^*(t), u_2^*)$ by applying the Pontryagin's maximum principle (PMP) ([28]) and reformulating (68), (69), (70), (71), (72), (73), and (75) into a problem of minimizing pointwise a Hamiltonian H, with respect to the control variables $(u_1(t), u_2(t))$. Hence, the Hamiltonian H is defined for all $t \in [0, T]$ by

$$\begin{aligned} &H(S_H(t), E_H(t), I_H(t), P_C(t), R_H(t), u_1(t), u_2(t),\\ &\quad \lambda_{S_H}(t), \lambda_{E_H}(t), \lambda_{I_H}(t), \lambda_{P_C}(t), \lambda_{R_H}(t))\\ &\quad = \left(\omega I_H + \frac{c_1}{2}u_1^2 + u_2^2\right) + \lambda_{S_H}[\lambda_h - \alpha(1-u_1(t))S_H I_H\\ &\qquad - \beta(1-u_1(t))S_H P_C - c_m S_H] + \lambda_{E_H}[\alpha(1-u_1(t))S_H I_H\\ &\qquad + \beta(1-u_1(t))S_H P_C - \theta E_H] + \lambda_{I_H}[\theta E_H - \gamma I_H - \psi_1 I_H\\ &\qquad - \tau I_H - u_2(t) I_H] + \lambda_{P_C}[(1-\varepsilon)\tau I_H - \psi_2 \nu P_C]\\ &\qquad + \lambda_{R_H}[\varepsilon\tau I_H + \psi_1 I_H + \psi_2 \eta P_C + u_2(t) I_H], \end{aligned} \tag{84}$$

where $\lambda_{S_H}, \lambda_{E_H}, \lambda_{I_H}, \lambda_{P_C}, \lambda_{R_H}$ represent the adjoint variables or costate variables. Next, we obtain the following using the Pontryagin maximum principle (PMP) and the existence result of the Filippov-Cesari theorem.

Lemma 10. *Suppose an optimal control u_1^* and u_2^* and the corresponding trajectories $S_H^*(t), E_H^*(t), I_H^*(t), P_C^*(t)$, and $R_H^*(t)$ of state systems (68), (69), (70), (71), (72), and (73) which minimize $J(u_1^*, u_2^*)$ over Ω. Then, there exist adjoint variables $\lambda_{S_H}(t)$, $\lambda_{E_H}(t)$, $\lambda_{I_H}(t)$, $\lambda_{P_C}(t)$, and $\lambda_{R_H}(t)$ which satisfy*

$$\begin{aligned} -\frac{d\lambda_{S_H}}{dt} &= \frac{\delta H}{\delta S_H} = -\lambda_H(-\alpha(1-u_1(t))I_H - \beta(1-u_1(t))P_C - c_m)\\ &\quad - \lambda_{E_H}(\alpha(1-u_1(t))I_H + \beta(1-u_1(t))P_C) - \frac{d\lambda_{E_H}}{dt}\\ &= \frac{\delta H}{\delta E_H} = -\lambda_{E_H}(-\theta) - \theta\lambda_{I_H} - \frac{d\lambda_{I_H}}{dt} = \frac{\delta H}{\delta I_H}\\ &= -\omega + \frac{\lambda_{S_H}\alpha(1-u_1)S_H}{N_H} - \lambda_{E_H}\alpha(1-u_1)S_H - \lambda_{I_H}\\ &\quad \cdot(-\gamma - \psi_1 - \tau - u_2(t)) - \lambda_{P_C}((1-\varepsilon)\tau)\\ &\quad - \lambda_{R_H}(\tau\varepsilon + \psi_1 - u_2(t)) - \frac{d\lambda_{P_C}}{dt} = \frac{\delta H}{\delta P_C}\\ &= \lambda_{S_H}\beta(1-u_1(t))S_H - \lambda_{S_H}\beta(1-u_1(t))S_H - \lambda_{P_C}\\ &\quad \cdot(-\psi_2\eta) - \psi_2\eta\lambda_{P_C} \end{aligned} \tag{85}$$

and with transversality conditions $\lambda_{S_H}(T) = \lambda_{E_H}(T) = \lambda_{I_H}(T) = \lambda_{P_C}(T) = \lambda_{R_H}(T) = 0$ and controls u_1^* and u_2^* satisfy the optimality conditions

$$\begin{aligned} u_1^* &= \max\left\{0, \min\left(1, \frac{\alpha I_H^* S_H^*(\lambda_{E_H} - \lambda_{S_H}) + \beta P_C^* S_H^*(\lambda_{E_H} - \lambda_{S_H})}{c_1}\right)\right\},\\ u_2^* &= \max\left\{0, \min\left(1, \frac{(\lambda_{I_H} - \lambda_{R_H})I_H}{c_2}\right)\right\}. \end{aligned} \tag{86}$$

Proof. We obtained the nonlinear system of differential equations for the adjoint variables by differentiating the Hamiltonian function (H), which is evaluated at the optimal control such that the adjoint/costate system is given by

$$\begin{aligned} -\frac{d\lambda_{S_H}}{dt} &= \frac{\partial H}{\partial S_H}\\ &= -\lambda_H(-\alpha(1-u_1(t))I_H - \beta(1-u_1(t))P_C - c_m)\\ &\quad - \lambda_{E_H}(\alpha(1-u_1(t))I_H + \beta(1-u_1(t))P_C - \frac{d\lambda_{E_H}}{dt}\\ &= \frac{\partial H}{\partial E_H} = -\lambda_{E_H}(-\theta) - \theta\lambda_{I_H} - \frac{d\lambda_{I_H}}{dt} = \frac{\partial H}{\partial I_H}\\ &= -\omega + \lambda_{S_H}\alpha(1-u_1)S_H - \lambda_{E_H}\alpha(1-u_1)S_H\\ &\quad - \lambda_{I_H}(-\gamma - \psi_1 - \tau - u_2(t)) - \lambda_{P_C}((1-\varepsilon)\tau)\\ &\quad - \lambda_{R_H}(\tau\varepsilon + \psi_1 - u_2(t)) - \frac{d\lambda_{P_C}}{dt} = \frac{\partial H}{\partial P_C}\\ &= \lambda_{S_H}\beta(1-u_1(t))S_H - \lambda_{S_H}\beta(1-u_1(t))S_H\\ &\quad - \lambda_{P_C}(-\psi_2\nu - \mu_h) - \psi_2\eta\lambda_{P_C}, \end{aligned} \tag{87}$$

and with transversality conditions $\lambda_{S_H}(T) = \lambda_{E_H}(T) = \lambda_{I_H}(T) = \lambda_{P_C}(T) = \lambda_{R_H}(T) = 0$ and the controls.

From the optimality condition

$$\frac{\partial H}{\partial u_1} = c_1 u_1 + \lambda_{S_H}[\alpha S_H I_H + \beta S_H P_C] + \lambda_{E_H}[-\alpha S_H I_H - \beta S_H P_C] = 0, \tag{88}$$

we obtain

$$u_1^* = \frac{\alpha I_H^* S_H^* (\lambda_{E_H} - \lambda_{S_H}) + \beta P_C^* S_H^* (\lambda_{E_H} - \lambda_{S_H})}{c_1}, \qquad \frac{\partial H}{\partial u_2} = c_2 u_2^* + \lambda_{I_H}[-I_H^*] + \lambda_{R_H}[I_H^*] = 0. \tag{89}$$

And we obtain

$$u_2^* = \frac{(\lambda_{I_H} - \lambda_{R_H}) I_H^*}{c_2}. \tag{90}$$

Then we have

$$u_1^* = \max\left\{0, \min\left(1, \frac{\alpha I_H^* S_H^* (\lambda_{E_H} - \lambda_{S_H}) + \beta P_C^* S_H^* (\lambda_{E_H} - \lambda_{S_H})}{N_H c_1}\right)\right\}, \tag{91}$$

$$u_2^* = \max\left\{0, \min\left(1, \frac{(\lambda_{I_H} - \lambda_{R_H}) I_H^*}{c_2}\right)\right\}. \tag{92}$$

To obtain the optimal control and the corresponding prevalence I_H, we therefore solve the following system

$$\begin{aligned}
\frac{dS_H}{dt} &= \lambda_h - \alpha(1-u_1(t))S_H I_H - \beta(1-u_1(t))S_H P_C - c_m S_H,\\
\frac{dE_H}{dt} &= \alpha(1-u_1(t))S_H I_H + \beta(1-u_1(t))S_H P_C - \theta E_H,\\
\frac{dI_H}{dt} &= \theta E_H - \gamma I_H - \psi_1 I_H - \tau I_H - u_2(t) I_H,\\
\frac{dP_C}{dt} &= (1-\varepsilon)\tau I_H - \psi_2 \nu P_C,\\
\frac{dR_H}{dt} &= \varepsilon\tau I_H + \psi_1 I_H + \psi_2 \nu P_C + u_2(t) I_H,
\end{aligned} \tag{93}$$

with initial conditions

$$\begin{aligned}
S_H(0) &= S_h^0 > 0,\\
E_H(0) &= E_H^0,\\
I_H(0) &= I_H^0(0) > 0,\\
P_C(0) &= P_C^0(0),\\
R_H(0) &= R_H^0(0) > 0,
\end{aligned} \tag{94}$$

$$-\frac{d\lambda_{S_H}}{dt} = g_1, \tag{95}$$

$$-\frac{d\lambda_{E_H}}{dt} = g_2, \tag{96}$$

$$-\frac{d\lambda_{I_H}}{dt} = g_3, \tag{97}$$

$$-\frac{d\lambda_{P_C}}{dt} = g_4, \tag{98}$$

$$-\frac{d\lambda_{R_H}}{dt} = g_5, \tag{99}$$

where

$$\begin{aligned}
g_1 &= -\lambda_H(-\alpha(1-u_1(t))I_H - \beta(1-u_1(t))P_C - c_m)\\
&\quad - \lambda_{E_H}(\alpha(1-u_1(t))I_H + \beta(1-u_1(t))P_C),\\
g_2 &= -\lambda_{E_H}(-\theta) - \theta\lambda_{I_H},\\
g_3 &= -\omega + \lambda_{S_H}\alpha(1-u_1)S_H - \lambda_{E_H}\alpha(1-u_1)S_H\\
&\quad - \lambda_{I_H}(-\gamma - \psi_1 - \tau - u_2(t)) - \lambda_{P_C}((1-\varepsilon)\tau)\\
&\quad - \lambda_{R_H}(\tau\varepsilon + \psi_1 - u_2(t)),\\
g_4 &= \lambda_{S_H}\beta(1-u_1(t))S_H - \lambda_{S_H}\beta(1-u_1(t))S_H\\
&\quad - \lambda_{P_C}(-\psi_2\eta) - \psi_2\eta\lambda_{P_C},\\
g_5 &= -\lambda_{R_H}(-\phi),
\end{aligned} \tag{100}$$

and with transversality conditions $\lambda_{S_H}(T) = \lambda_{E_H}(T) = \lambda_{I_H}(T) = \lambda_{P_C}(T) = (T) = 0$ where u_1^* and u_2^* are given by (91) and (92). We cannot solve systems (95), (96), (97), (98), and (99) manually but numerical methods must be employed.

We hereby present the numerical solution of the optimality system and its corresponding optimal control pairs, the parameter values, and the various scenarios and interpretation in the next section.

6. Numerical Results

In this section, we present our numerical findings based on the optimal transmission parameter control measures for the COVID-19 dynamic model. We obtained the optimal control by solving the optimality system which involves the nonlinear differential equations (state equation) and the adjoint or costate equations. We applied the iterative scheme to solve the optimality system, and using the fourth-order Runge-Kutta method, we start to solve the state equations while we guess for the control measures over the simulated time. We solved the adjoint equations by a backward fourth-order Runge-Kutta scheme using the present iterative solutions of the state equation because of the transversality conditions. We employed a convex combination of the previous controls to update the controls and the value from the

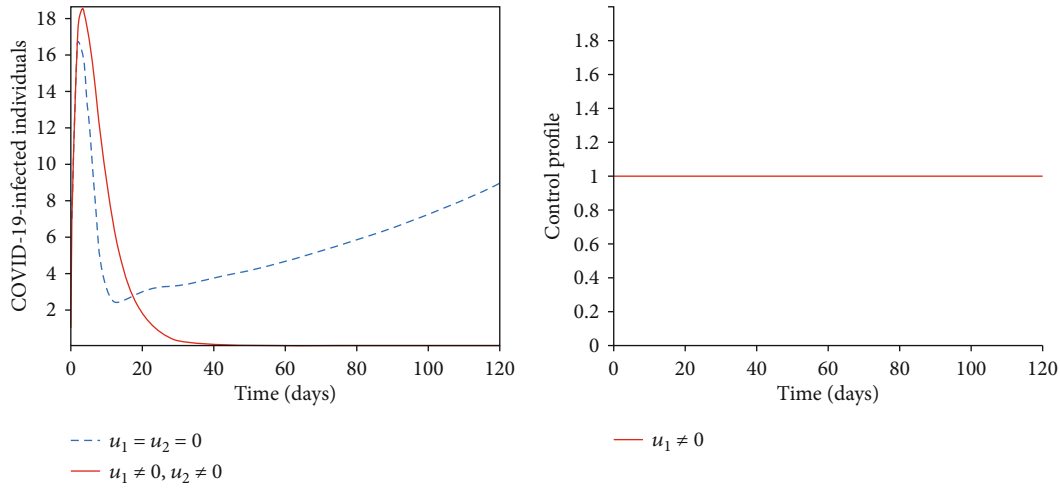

FIGURE 10: Simulations showing the effect of social distancing only on infected human (I_h) in Figure 10(a) and the control profile in Figure 10(b).

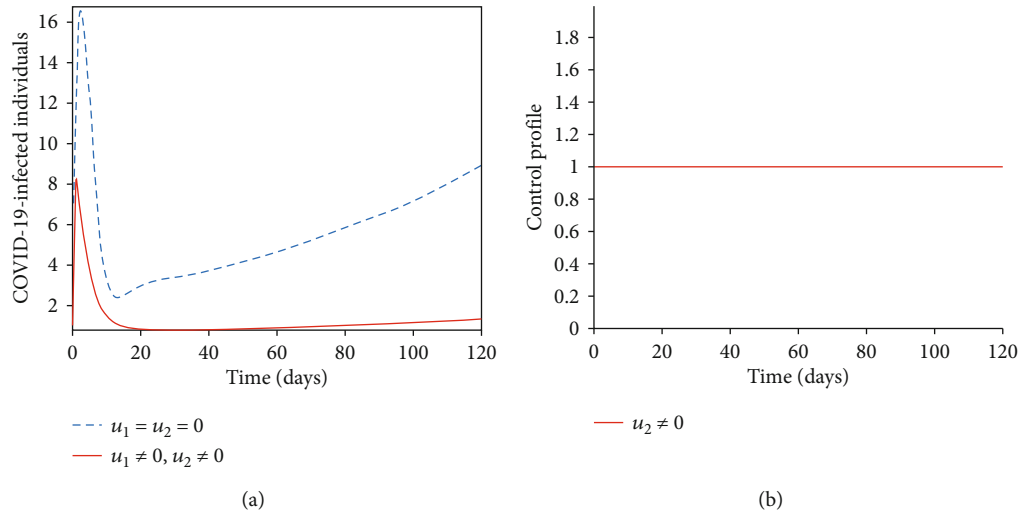

FIGURE 11: Simulations showing the effect of treatment only on infected human (I_h) in Figure 11(a) and the control profile in Figure 11(b).

characterizations of the optimality conditions. We repeat the process, and iterations are truncated if the values of the unknowns at the preceding iteration are near to the present iterations ([29]). A COVID-19 model with preventive and treatment as control measures was investigated to predict the effects of control practices and the transmission of COVID-19. Building various scenarios of the two control measures either one control measure at a time or two control measures at a time, we examine and compare numerical results from simulations using the following scenarios.

(1) Strategy A: employing social distancing (u_1) without treatment $(u_2 = 0)$

(2) Strategy B: treatment of the symptomatic individuals (u_2) without using social distancing $(u_1 = 0)$

(3) Strategy C: employing all the two control measures (u_1, u_2)

The parameter values are given in Tables 1 and 3, and we obtained the optimal control strategy by the forward-backward sweep Runge-Kutta method of order 4. The weight constants $\omega = 500$, $c_1 = 200$, and $c_2 = 200$. We ran the simulations for $T = 1{,}000$ days, and the results from the simulations with parameters in Table 3 are presented in Figures 10, 11, and 12.

In strategy A, we use only the control measure (u_1) to optimize the objective functional J, while the control measure on treatment (u_2) is set to zero. The results in Figure 10(a) reveal that the control strategy provide a decrease in the number of symptomatic human (I_H) as against the increase in the uncontrolled case. The control

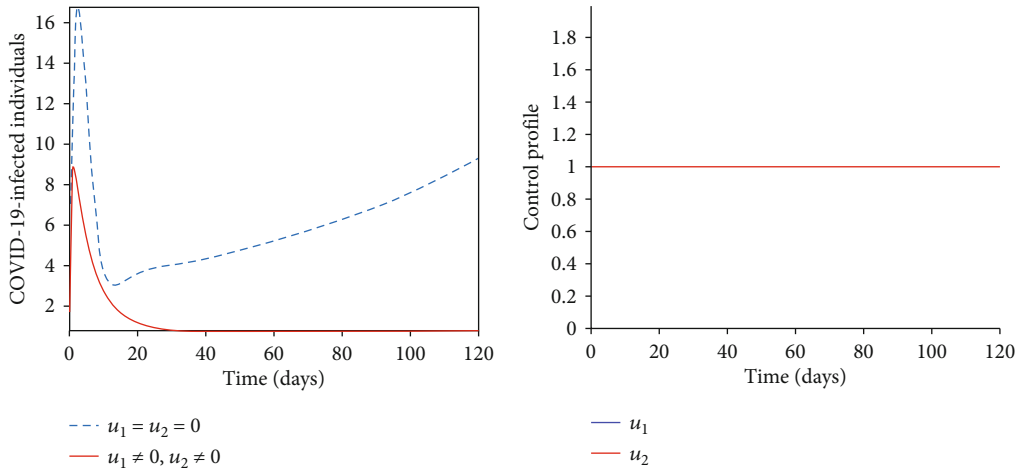

FIGURE 12: Simulations showing the effect of social distancing and treatment on infected human (I_h) in Figure 12(a) and the control profile in Figure 12(b).

profile is presented in Figure 10(b), where the optimal social distancing control (u_1) remains constant till the final time.

Applying this strategy B, we employed the treatment control measure only (u_2) while we set the control on social distancing (u_2) to zero. We observed that Figure 11(a) showed that effective treatment only has significant impact in decreasing COVID-19 incidence in the population, while the control profile in Figure 11(b) showed also that the control remains constant till the final time.

In strategy C, we applied the two controls (u_1, u_2), to optimise the objective functional J. For this strategy, in Figure 12(a), it was observed that the control strategy had significant impact in reducing the number of symptomatic humans as against the increased number of cases under the uncontrolled case. The control profile in Figure 12(b) showed also that the control remains constant till the final time.

7. Conclusion

Hence, we presented a COVID-19 model with partially recovered carriers. We investigated the stability of the model which revealed that the disease-free equilibrium is locally and globally asymptotically stable. Scatter plots and the tornado plots of the parameters in R_c (reproduction number) revealed that the contact rate between susceptible and infectious individuals (α) has a major impact on the transmission of COVID-19 disease, followed by the transmission rate from the exposed to infectious class, θ. This supports the fact that since the transmission rate is very high, the disease can spread fast in the population. We also observed from our results that the influence of the partially recovered contact rate is lower compared to the contact rate between susceptible and infectious individuals. The scenarios built on the optimal control strategies showed that the use of social distancing and treatment are the best option to control the disease in that they reduce the impact of the epidemic in the community and slows down the epidemic curve. Other interesting modeling works can be found in [30, 31]. The developed models predicted the reduction and control of COVID-19 through incorporating multiple control interventions.

Data Availability

The data used to support the findings of this study are included within the article. The authors used a set of parameter values whose sources are from the literature and others are estimated depending on the epidemiology of COVID-19 in Nigeria as shown in Table 1.

Conflicts of Interest

The authors declare that they have no conflicts of interest.

Acknowledgments

The second author would like to thank the Faculty of Science in the Federal University Oye Ekiti, Ekiti State, Nigeria. All authors would like to thank the Faculty of Basic Medical and Applied Sciences in Lead City University, Ibadan, Oyo state, Nigeria.

References

[1] D. S. C. Hui and A. Zumla, "Severe acute respiratory syndrome: historical, epidemiologic, and clinical features," *Infectious Disease Clinics of North America*, vol. 33, no. 4, pp. 869–889, 2019.

[2] E. de Wit, N. Van Doremalen, D. J. Falzarano, and V. J. Munster, "SARS and MERS: recent insights into emerging coronaviruses," *Nature Reviews Microbiology*, vol. 14, no. 8, pp. 523–534, 2016.

[3] K. H. Kim, T. E. Tandi, J. W. Choi, J. M. Moon, and M. S. Kim, "Middle East respiratory syndrome coronavirus (MERS-Cov) outbreak in South Korea, 2015: epidemiology, characteristics and public health implications," *The Journal of Hospital Infection*, vol. 95, no. 2, pp. 207–213, 2017.

[4] I. I. Bogoch, A. Watts, A. Thomas-Bachli, C. Huber, M. U. G. Kraemer, and K. Khan, "Pneumonia of unknown aetiology in Wuhan, China: potential for international spread via commercial air travel," *Journal of Travel Medicine*, vol. 27, no. 2, 2020.

[5] S. Zhao, Q. Lin, J. Ran et al., "Preliminary estimation of the basic reproduction number of novel coronavirus (2019-ncoV) in China, from 2019 to 2020: a data-driven analysis in the early phase of the outbreak," *International Journal of Infectious Diseases*, vol. 92, pp. 214–217, 2020.

[6] "Coronavirus: the first three months as it happened," https://www.nature.com/articles/d41586-020-00154.

[7] L.-L. Ren, Y.-M. Wang, Z.-Q. Wu et al., "Identification of a novel coronavirus causing severe pneumonia in human: a descriptive study," *Chinese Medical Journal*, vol. 133, no. 9, pp. 1015–1024, 2020.

[8] M. Egger, L. Johnson, C. Althaus et al., "Developing WHO guidelines: time to formally include evidence from mathematical modelling studies," *F1000 Research*, vol. 6, article 1584, 2017.

[9] T. Biao, N. Luigi Bragazzi, Q. Li, S. Tang, Y. Xiao, and J. Wu, "An updated estimation of the risk of transmission of the novel coronavirus (2019-nCov)," *Infectious Disease Modeling*, vol. 5, pp. 248–255, 2020.

[10] T. Chen, J. Rui, Q. Wang, Z. Zhao, J. A. Cui, and L. A. Yin, *A Mathematical Model for Simulating the Transmission of Wuhan Novel Coronavirus*, bioRxiv, 2020.

[11] K. Hattaf and N. Yousfi, "Dynamics of SARS-COV-2 infection model with two modes of transmission and immune response," *Mathematical Biosciences and Engineering*, vol. 17, no. 5, pp. 5326–5340, 2020.

[12] N. Imai, I. Dorigatti, A. Cori, C. Donnelly, S. Riley, and N. M. Ferguson, *Report 2: Estimating the Potential Total Number of Novel Coronavirus Cases in Wuhan City, China*, January 2020, https://www.imperial.ac.uk/media/imperial-college/medicine/sph/ide/gida-fellowships/2019-nCov-outbreak-report-22-01-2020.pdf.

[13] A. A. Mohsen, H. F. AL-Hussein, X. Zhou, and K. Hattaf, "Global stability of Covid-19 model involving the quarantine strategy and media coverage effects," *AIMS Public Health*, vol. 7, no. 3, pp. 587–605, 2020.

[14] L. N. Nkamba, M. L. Mann Manyombe, T. T. Manga, and J. Mbang, *Modeling Analysis of a SEIQR Epidemic Model to Assess the Impact of Undetected Cases and Containment Measures of the COVID-19 Outbreak in Cameroon*, London Journal Press, 2020.

[15] B. Tang, X. Wang, Q. Li et al., "Estimation of the transmission risk of the 2019-nCov and its implication for public health interventions," *Journal of Clinical Medicine*, vol. 9, no. 2, p. 462, 2020.

[16] C. Tian-Mu, J. Rui, W. Qui-Peng, Z. Za-Yu, C. Jing-An, and Y. Ling, "A mathematical model for simulatiing the phase-based transmissibility of a novel coronavirus," *Infectious Disease of Poverty*, vol. 9, p. 24, 2020.

[17] M. A. Khan, A. Atangana, E. Alzahrani, and Fatmawati, "The dynamics of COVID-19 with quarantined and isolation," *Advances in Difference Equations*, vol. 2020, no. 1, 2020.

[18] M. Awais, F. S. Alshammari, S. Ullah, M. A. Khan, and S. Islam, "Modeling and simulation of the novel coronavirus in Caputo derivative," *Results in Physics*, vol. 19, article 103588, 2020.

[19] L. Lan, D. Xu, G. Ye et al., "Positive RT-PCR test results in patients recovered from COVID-19," *The Journal of the American Medical Association*, vol. 323, no. 15, pp. 1502-1503, 2020.

[20] S. Pappas, *Can People Spread Coronavirus after They Recover?*, Live Science Contributor, 2020.

[21] O. Diekmann, J. A. P. Heesterbeek, and J. A. J. Metz, "On the definition and the computation of the basic reproduction ratio R_0 in models for infectious diseases in heterogeneous populations," *Journal of Mathematical Biology*, vol. 28, no. 4, pp. 365–382, 1990.

[22] P. Lancaster, *Theory of Matrices*, Academic Press, New York, NY, USA, 1969.

[23] J. P. LaSalle, *The Stability of Dynamical Systems*, SIAM, 1976.

[24] H. Guo and M. Y. Li, "Global stability in a mathematical model of tuberculosis," *Canadian Applied Mathematics Quaterly*, vol. 14, no. 2, 2006.

[25] N. Chitnis, J. M. Hyman, and J. M. Cushing, "Determining important parameters in the spread of malaria through the sensitivity analysis of a mathematical model," *Bulletin of Mathematical Biology*, vol. 70, no. 5, pp. 1272–1296, 2008.

[26] M. Martcheva, "An introduction to mathematical epidemiology," in *Texts in Applied Mathematics*, Springer, 2015.

[27] A. Seierstad and K. Sydseter, *Optimal Control Theory with Economic Applications, vol. 24 of Advanced Textbooks in Economics*, North-Holland Publishing Co., Amsterdam, 1987.

[28] L. S. Pontryagin, V. G. Boltyanskii, R. V. Gamkrelidze, and E. F. Mishchenko, *The Mathematical Theory of Optimal Processes*, Wiley, New York, NY, USA, 1962.

[29] S. Lenhart and J. T. Workman, *Optimal Control Applied to Biological Models*, Chapman and Hall, 2007.

[30] K. Hattaf and H. Dutta, "Modeling the dynamics of viral infections in presence of latently infected cells," *Chaos, Solitons & Fractals*, vol. 136, article 109916, 2020.

[31] M. A. Khan and A. Atangana, "Modeling the dynamics of novel coronavirus (2019-nCov) with fractional derivative," *Alexandria Engineering Journal*, vol. 59, no. 4, pp. 2379–2389, 2020.